SANDIA REPORT

SAND2010-6943
Unlimited Release
Printed December 2010

The Sandia MEMS Passive Shock Sensor: Dormancy and Aging

Michael S. Baker and Danelle M. Tanner

Prepared by
Sandia National Laboratories
Albuquerque, New Mexico 87185 and Livermore, California 94550

Sandia National Laboratories is a multi-program laboratory managed and operated by Sandia Corporation, a wholly owned subsidiary of Lockheed Martin Corporation, for the United States Department of Energy's National Nuclear Security Administration under Contract DE-AC04-94AL85000.

Approved for public release; further dissemination unlimited.

Sandia National Laboratories

Issued by Sandia National Laboratories, operated for the United States Department of Energy by Sandia Corporation.

NOTICE: This report was prepared as an account of work sponsored by an agency of the United States Government. Neither the United States Government, nor any agency thereof, nor any of their employees, nor any of their contractors, subcontractors, or their employees, make any warranty, express or implied, or assume any legal liability or responsibility for the accuracy, completeness, or usefulness of any information, apparatus, product, or process disclosed, or represent that its use would not infringe privately owned rights. Reference herein to any specific commercial product, process, or service by trade name, trademark, manufacturer, or otherwise, does not necessarily constitute or imply its endorsement, recommendation, or favoring by the United States Government, any agency thereof, or any of their contractors or subcontractors. The views and opinions expressed herein do not necessarily state or reflect those of the United States Government, any agency thereof, or any of their contractors.

Printed in the United States of America. This report has been reproduced directly from the best available copy.

Available to DOE and DOE contractors from
U.S. Department of Energy
Office of Scientific and Technical Information
P.O. Box 62
Oak Ridge, TN 37831

Telephone: (865)576-8401
Facsimile: (865)576-5728
E-Mail: reports@adonis.osti.gov
Online ordering: http://www.osti.gov/bridge

Available to the public from
U.S. Department of Commerce
National Technical Information Service
5285 Port Royal Rd
Springfield, VA 22161

Telephone: (800)553-6847
Facsimile: (703)605-6900
E-Mail: orders@ntis.fedworld.gov
Online order: http://www.ntis.gov/help/ordermethods.asp?loc=7-4-0#online

SAND2010-6943
Unlimited Release
Printed December 2010

The Sandia MEMS Passive Shock Sensor: Dormancy and Aging

Michael S. Baker
Org. 1749-2, Advanced MEMS

Danelle M. Tanner
Org. 1732, Frequency Devices and Capacitors

Sandia National Laboratories
P.O. Box 5800
Albuquerque, NM 87185-1310

Abstract

This report presents the results of an aging experiment that was established in FY09 and completed in FY10 for the Sandia MEMS Passive Shock Sensor. A total of 37 packages were aged at different temperatures and times, and were then tested after aging to determine functionality. Aging temperatures were selected at 100 C and 150 C, with times ranging from as short as 100 hours to as long as 1 year to simulate a predicted aging of up to 20 years. In all of the tests and controls, 100% of the devices continued to function normally.

Acknowledgment

The authors would like to thank Lauren Watts and Charlie Cook at the Kansas City Plant for their work in residual gas analysis, and the Sandia NM org. 1715 packaging department for their assistance with the wire pull and die shear tests.

Table of Contents

1. Introduction 7
2. Arrhenius Acceleration Model 7
3. Design of Experiments 8
4. Test Results 10
   4.1. Functionality Testing 11
   4.2. Resistance Measurements 12
   4.3. Residual Gas Analysis 12
   4.4. Wire Pull, Die Shear and Package Shear Tests 15
5. Conclusions 16
6. References 16

List of Figures

Figure 3-1: Plot showing predicted aging as a function of test time and temperature 9
Figure 3-2: Photograph of the test oven with packages inside. 10

List of Tables

Table 3-1: Test matrix of time, temperature, and predicted aging 8
Table 4-1: List of all test conditions and part status 10
Table 4-2: Contact resistance before and after each experiment. 12
Table 4-3: RGA results for 100 C experiments. Units are ppmv unless otherwise noted. 13
Table 4-4: RGA results for 150 C experiments and control devices. Units are ppmv unless otherwise noted. 14
Table 4-5: Wire pull and die shear for 100 C experiments. Die shear is in kilograms force, wire pull is in grams force. 15
Table 4-6: Wire pull and die shear for 150 C experiments and control devices. Die shear is in kilograms force, wire pull is in grams force. 15

1. Introduction

This report presents the results of an aging experiment that was established in FY09 and completed in FY10 for the Sandia MEMS Passive Shock Sensor. The passive shock sensor device is described in detail in [1], with a discussion of the aging framework presented in section 6, pages 50-57. As part of the maturation of the shock sensor design, it is important to understand how aging and dormancy might affect device performance. Particular mechanisms of degradation that may be of concern include:

1. JM7000 out-gassing in package leading to contamination of contacts or device.
2. Aged JM7000 as it relates to shear strength of the die.
3. Wire bond lifting (Au/Au or Au/Pt)
4. Switch contact resistance increasing over time.
5. LCC-PCB solder joint strength.
6. Package hermeticity and moisture content.

In order to address these concerns an accelerated aging experiment was performed on a total of 37 packaged parts, with 7 control parts. Contact resistance was measured before and after aging for all devices, and at the end of the aging cycle parts were selected for additional destructive testing to determine quantitative parameters that might help address the concerns listed above. For example, residual gas analysis (RGA) was performed to measure package hermeticity, and wire bond strength, die shear strength, and package shear strength was measured on a sample of parts.

2. Arrhenius Acceleration Model

In order to evaluate these reliability concerns in the context of long-term aging of the part, a method of time acceleration must be used. While discussed in [1], the Arrhenius acceleration model is described again here for completeness. The aging study presented in this work use a model with time and temperature as the only variables. With this approach, components are exposed to elevated temperatures for extended periods of time to simulate an accelerated aging condition. After exposure to this simulated aging environment, components are removed from the environment and failures are investigated. The model assumes that failures are driven by thermal processes that can be modeled using the Arrhenius equation, which is well suited to modeling many thermally activated processes.

The empirical equation that has been successfully used to model thermal acceleration is shown below.

$$TF = Ae^{-E_{aa}/k_b T} \tag{1}$$

where TF is time to failure, A is an unknown constant, E_{aa} is the apparent activation energy in eV, k_b is Boltzmann's constant, 8.62 x 10^{-5} eV/Kelvin, and T is temperature in Kelvin. The acceleration factor, AF, for a given failure mechanism is then defined as the ratio of the time to failure at the use temperature (T_1), to the time to failure at an elevated temperature (T_2). Using Eq. 1, the acceleration factor, AF for T_1 vs. T_2 is as follows:

$$AF = e^{(E_{aa}/k_b)(1/T_1 - 1/T_2)} \quad (2)$$

Note that the unknown constant *A* cancels when the ratio of time to failure is taken, leaving only the apparent activation energy and the test temperature as unknowns. In a practical experiment, this acceleration factor, *AF*, is used to predict operating life by aging a device at a temperature T_2 for a specified test time and then determining if the part has failed. If no failure is detected then the life at operating temperature T_1 is assumed to be greater than the test time multiplied by the acceleration factor. If a failure is observed then the life is assumed to be less than the test time multiplied by the acceleration factor, with the precise lifetime unknown.

The MEMS shock sensor is a "microelectronics" component with aging issues that relate to die attach, wire-bonding, hermeticity, and material out-gassing. The mechanisms of concern can be interrelated, but may have different acceleration factors depending upon temperature. Failure mechanisms associated with some of these processes have been documented in several JEDEC (standards) publications [2] along with ranges of "Apparent Activation Energies" used for modeling these failures. Most activation energies listed are > 0.7 eV. To know the true apparent activation energy for a particular failure mechanism would require extensive time-to-failure data at various temperatures, which is time intensive and expensive to obtain. For this reason, the framework presented here uses the conservative "industry standard" of E_{aa} = 0.7eV. If failures are observed in the experiments, then E_{aa} < 0.7eV and the acceleration factor would have to be re-calculated. However, if there are no failures then E_{aa} > 0.7eV and aging from thermal environments can be predicted.

3. Design of Experiments

Six different combinations of time and temperature were selected for this set of experiments in order to map out the predicted aging of this device to greater than 20 years. This matrix is outlined in Table 3-1, and is shown graphically in Figure 3-1, assuming an apparent activation energy of 0.7eV as discussed in Section 2. The test temperatures were higher than the maximum operating temperature of 50C to accelerate aging, but not so high as to activate other failure mechanisms.

Table 3-1: Test matrix of time, temperature, and predicted aging.

Experiment Number	Temperature (C)	Time (Hours)	Predicted Aging (yrs)	Number of Parts Tested	Design Revision
1	100	1000	3.3	5	Rev7
2	100	3000	10.0	5	Rev7
3	100	6000	20.1	5	Rev7
4	100	8766	29.3	6	Rev7
5	150	100	4.4	8	Rev6
6	150	500	22.1	8	Rev6
100 C Controls				3	Rev7
150 C Controls				4	Rev6

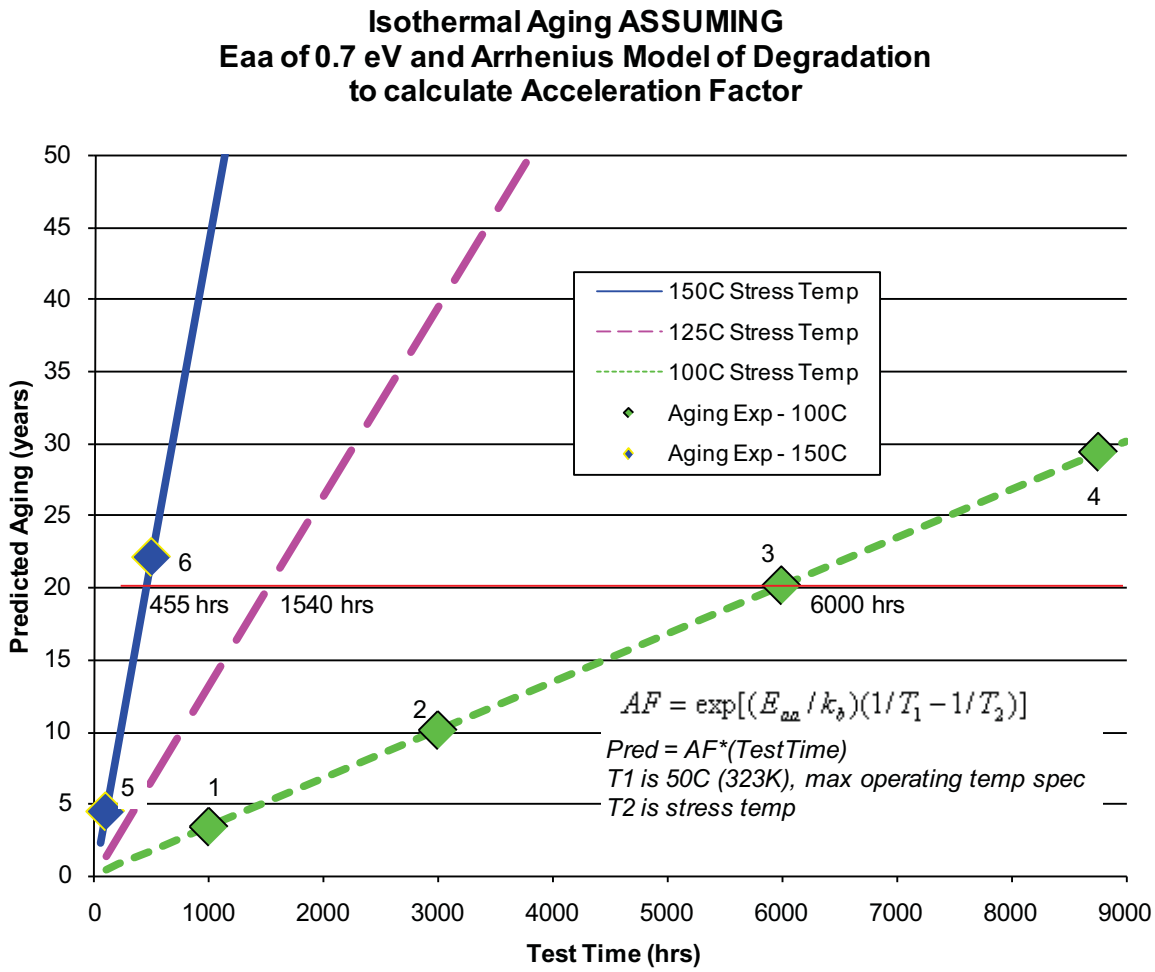

Figure 3-1: Plot showing predicted aging as a function of test time and temperature.

For a detailed description of the differences between design revisions 6 and 7 see the previous SAND reports on this project [1], however for the purposes of this experiment they both use the same packaging procedure with the same die attach, Aluminum wire bond, and solder lid seal. They also have nominally the same Platinum contact metallization.

All of the devices were self-tested to verify functionality and to record a starting contact resistance value before being placed in the test ovens. Each package contains a die with four different shock switch devices, so four contact resistance values can be monitored in each package. A photo of the test oven with parts inside is shown in Figure 3-2.

For each of the 6 different experiments (where each experiment represents a time and temperature combination), half of the devices under test were aged with the contacts in the closed position, and half with the contacts left in the open position.

Figure 3-2: Photograph of the test oven with packages inside.

4. Test Results

A summary of functionality testing results, along with a description of the contact state and post-test destructive testing performed on each design is listed in Table 4-1.

Table 4-1: List of all test conditions and part status

Experiment	Build	Package ID	Initial Functioning Devices	Contact Status During Test	Test Results	D-Test
1	7_1	5025	ABCD	open	All OK	RGA
100C 1000hr	7_1	5026	ABCD	closed	All OK	Shear/Pull
	7_1	5027	ABCD	open	All OK	Shear/Pull
	7_1	5028	ABCD	closed	All OK	Shear/Pull
	7_1	5030	ABCD	open	All OK	RGA
2	7_1	5031	ABCD	open	All OK	RGA
100C 3000hr	7_1	5032	ABCD	closed	All OK	Shear/Pull
	7_1	5033	ABCD	open	All OK	
	7_1	5034	ABCD	closed	All OK	Shear/Pull
	7_1	5035	ABCD	open	All OK	RGA
3	7_1	5036	ABCD	open	All OK	RGA
100C 6000hr	7_1	5037	ABCD	closed	All OK	Shear/Pull
	7_1	5038	ABCD	open	All OK	

Experiment	Build	Package ID	Initial Functioning Devices	Contact Status During Test	Test Results	D-Test
	7_1	5039	ABCD	closed	All OK	Shear/Pull
	7_1	5041	ABCD	open	All OK	RGA
4	7_1	5042	ABCD	open	All OK	RGA
100C 1yr	7_1	5043	ABCD	closed	All OK	RGA
	7_1	5044	ABCD	open	All OK	Shear/Pull
	7_1	5045	ABCD	closed	All OK	
	7_1	5048	ABCD	open	All OK	
	7_1	5049	ABCD	closed	All OK	Shear/Pull
5	6_2	1231	ABCD	open	All OK	pkg x-sec
150C 100hr	6_2	1232	ABCD	closed	All OK	Shear/Pull
	6_2	1235	CD	open	BCD OK	Shear/Pull
	6_2	1236	ABCD	closed	All OK	Shear/Pull
	6_2	1238	ABCD	open	All OK	RGA
	6_1	1214	ABCD	closed	All OK	RGA
	6_1	1217	ABCD	open	All OK	Shear/Pull
	6_1	1218	ABCD	closed	All OK	pkg x-sec
6	6_2	1239	ABCD	open	All OK	
150C 500hr	6_2	1240	ABCD	closed	All OK	
	6_2	1241	ABCD	open	All OK	
	6_2	1242	ABCD	closed	All OK	Shear/Pull
	6_2	1243	ABCD	open	All OK	RGA
	6_1	1221	ABCD	closed	All OK	RGA
	6_1	1222	ACD	open	ACD OK	Shear/Pull
	6_1	1228	ABCD	closed	All OK	
Controls	6_2	1244	BCD	open	All OK	RGA
150C	6_2	1245	ABCD	closed	All OK	Shear/Pull
	6_1	1215	ABCD	open	All OK	Shear/Pull
	6_1	1216	ABCD	closed	All OK	pkg x-sec
Controls	7_1	5029	ACD	open	ACD OK	RGA
100C	7_1	5040	BCD	closed	BCD OK	Shear/Pull
	7_1	5047	ABCD	open	All OK	Shear/Pull

4.1. Functionality Testing

All devices were self-tested at the beginning and end of the thermal aging experiment. The control devices were also tested after each batch of parts was removed from the test ovens for comparison. A self-test failure was never recorded in any of the tests, of both the aged parts and the controls. There were five packages that had less than all four devices functioning at the very first test, these failures are considered to be yield-loss and are not due to any aging

or thermal stress the parts saw during testing. But no additional failures were recorded as a result of the aging experiments.

In two devices (parts 1235, experiment 5 and part 1244, control) one device that was not initially functioning began to operate properly during subsequent testing. Because this happened on one aged device and one control it cannot be attributed solely to the thermal aging that the parts experienced.

4.2. Resistance Measurements

The closed contact resistance of each device was measured before and after each experiment to determine if a change in contact resistance can be expected during aging conditions. While contact resistance increases have been observed after a large number of open-close cycles on this device, this is the first experiment to determine if aging without cycling will negatively affect contact performance. The average contact resistance before and after each experiment is shown in Table 4-2 with the data separated based on the contact position during the experiment.

Table 4-2: Contact resistance before and after each experiment.

	Device Left Open During Test		Device Left Closed During Test	
Experiment	Before (Ω)	After (Ω)	Before (Ω)	After (Ω)
100 C, 1000 hrs	52.1	55.3	51.3	50.7
100 C, 3000 hrs	50.7	52.5	51.8	49.7
100 C, 6000 hrs	50.0	51.8	51.1	49.4
100 C, 1 yr	50.9	51.7	49.8	48.4
150 C, 100 hrs	45.6	No Data	42.0	41.0
150 C, 500 hrs	44.0	49.5	46.8	44.0
Controls	51.1		45.9	

The maximum recorded resistance in any test was 62.8 Ω, and the minimum was 35.0 Ω. In examining this data it can be seen that the contact resistance of devices aged with the contacts left open showed a slight increase, while contacts aged in the closed position showed a slight decrease in resistance. This trend is very consistent across all experiments, but the magnitude of the change is quite small, and is within the observed variation in resistance that is seen from one contact closure to the next at ambient.

It is important to note that the failure mechanisms related to micro-scale low-force platinum contacts is not well understood. As such, elevating the temperature may not necessarily act as an acceleration factor.

4.3. Residual Gas Analysis

Fourteen shock sensor packages were analyzed at the Kansas City Plant (KCP) by Residual Gas Analysis (RGA). The RGA is a Pernicka Corporation RGA with a quadrapole mass spectrometer that scans from 2 to 150 atomic mass units (amu). There are 5 background scans prior to sample being introduced and 20 scans of the gas sample that are analyzed for each run.

The RGA is calibrated for moisture using a bottle of dry nitrogen that is swept into a moisture generator, across a chilled mirror and a MCM Moisture Monitor (calibrated by KCP metrology). The moisture reading from the moisture monitor is used as a verification that the chilled mirror is working properly before proceeding with analysis. The moist nitrogen gas is then used as a standard to calibrate the readings from the RGA. The gas is analyzed at least three times to ensure stability of the instrument.

The RGA is also calibrated for fixed gases and hydrocarbons using a 100ppm standard of Hydrogen, Carbon Monoxide, Carbon Dioxide, Argon and Oxygen with 6% Helium and a balance of Nitrogen and a hydrocarbon standard with 1500 ppm Methane, 3150 ppm other hydrocarbons, 12% Argon with a balance of Nitrogen. These standards are not run through the moisture generator, but are swept across the chilled mirror and the Moisture Monitor. The standards are analyzed at least three times each to ensure stability of the instrument.

The shock sensor packages were analyzed by placing them onto the RGA stage and sealing against an o-ring to the inlet system. The samples were conditioned prior to sampling for 16-24 hours at 100 C and were sampled at 100 C. The connectors of each switch were removed prior to analysis so they could fit against the o-ring.

Results for all tested packages are shown in Table 4-3 and Table 4-4. Measurements that are significantly different from the average are highlighted. Values are given in ppmv except for Nitrogen content which is given as a percent, and pressure in Torr. For reference 10,000 ppmv equals 1% by volume.

Table 4-3: RGA results for 100 C experiments. Units are ppmv unless otherwise noted.

Test Condition	**100 C 1000 hrs**		**100 C 3000 hrs**		**100 C 6000 hrs**		**100 C 1 yr**	
Package ID	**5025**	**5030**	**5031**	**5035**	**5036**	**5041**	**5042**	**5043**
Hydrogen	1505	1635	1341	4	1252	1413	1319	2427
Helium	13	5	12	31	1	2	2	1
Methane	151	112	138	166	78	90	89	92
Water	4030	2904	1499	**20930**	1159	2320	1263	4472
Neon	0	0	0	0	7	10	5	18
Nitrogen (%)	99.176	99.359	99.523	**96.115**	99.587	99.431	99.555	99.121
CO	131	136	127	109	106	105	100	108
Oxygen	80	59	62	**3263**	32	58	37	52
Argon	908	726	743	**12712**	384	436	413	421
CO2	1309	721	744	1277	1025	1166	1110	1081
HC/Organics	36	60	74	14	87	88	102	113
Fluorocarbons	4	2	3	2	4	6	5	6
NH3	72	51	24	340	0	0	0	0
Pressure (torr)	0.1381	0.1623	0.1633	**0.1943**	0.1643	0.1580	0.1627	0.1610

Table 4-4: RGA results for 150 C experiments and control devices. Units are ppmv unless otherwise noted.

Test Condition	**150 C 100 hr**		**150 C 500 hr**		**Controls**	
Package ID	**1238**	**1214**	**1243**	**1221**	**5029**	**1244**
Hydrogen	4	5	0	0	2135	0
Helium	5	19	0	1	4	2
Methane	106	144	65	71	71	63
Water	4084	**13137**	4106	2890	724	4233
Neon	0	0	20	9	3	17
Nitrogen (%)	99.3313	**96.9312**	99.3523	99.4998	99.6032	99.4652
CO	143	111	106	106	100	104
Oxygen	166	**3360**	70	64	21	76
Argon	1230	**12765**	453	480	407	476
CO2	848	887	1600	1295	443	357
HC/Organics	24	13	48	65	51	15
Fluorocarbons	2	2	8	21	9	5
NH3	75	246	0	0	0	0
Pressure (torr)	0.1688	**0.1939**	0.1651	0.1627	0.1635	0.1537

All packages were hermetically sealed, and there were no indications of any leaks. Packages 5035 and 1214 are highlighted in the Tables as being different from the other packages. They had significantly higher water, oxygen and argon content, and a higher inlet pressure during the RGA test. This does not seem to be an effect of temperature cycling but rather some difference in the initial state of these two packages. For example, if the package were not properly cleaned or dried the excess moisture in the package during sealing could explain the higher pressure and water levels observed.

There are few trends that can be identified as being related to the aging time and temperature. All devices tested at 150 C showed very low Hydrogen content of 5 ppm or less, while most packages tested at 100 C showed 1200-1600 ppm. Package 5035 is the only exception to this trend, but given its anomalous measurements in other areas it may be reasonable to ignore this data point. However, the two control devices somewhat invalidate this observed trend because one of them shows 0 ppm hydrogen while the other has the second highest level of any device tested. So it is difficult to conclude that this trend is significant, or due to the thermal aging.

A similar trend is observed in the hydro-carbon/organics measurement. In general this value appears to increase with time at elevated temperatures. However, given the variation in this measurement compared to the variation in the control samples, it is difficult to draw a definitive conclusion.

A final observed trend relates to the quantity of CO2, which tends to increase with time and temperature. In this case the control samples are consistent with this trend, and CO2 is a known byproduct of reaction with moisture and un-reacted species in the JM7000 die attach

adhesive. However, water vapor levels are still quite high, which may indicate that the JM7000 is already fully cured due to the extended cure cycle used. While all the packages except for 1214 and 5035 show water levels below the MIL-STD-883-G requirement of 5000 ppmv, levels are significantly higher than the desired target of 1000 ppmv for MEMS devices. See Section 6.6 in [1] for more discussion on MEMS hermeticity.

4.4. Wire Pull, Die Shear and Package Shear Tests

After performing functional testing, two devices from each test condition were destructively wire-pull tested and die shear tested. According to MIL-STD-883-G, for the 1 mil diameter Aluminum wire used in these devices the post-lid-seal minimum bond pull strength is 1.5 grams force. For the die size used, the minimum allowable die shear strength is 2.5 kilograms force, or 5 kilograms force if the failure shows less than 75% adhesion across the die area. A summary of the test results is shown in Table 4-5 and Table 4-6. For each device, there were 18 wire bonds tested.

Table 4-5: Wire pull and die shear for 100 C experiments. Die shear is in kilograms force, wire pull is in grams force.

Test Condition	**100 C 1000 hrs**		**100 C 3000 hrs**		**100 C 6000 hrs**		**100 C 1 yr**	
Package ID	**5027**	**5028**	**5032**	**5034**	**5037**	**5039**	**5044**	**5049**
Die Shear	19.5	22.4	23.9	21.9	22.2	27.0	20.8	20.7
Min wire pull	2.21	2.79	2.64	2.35	3.19	2.89	2.74	3.20
Max wire pull	4.32	4.52	4.84	4.74	4.75	4.41	4.24	4.72
Average pull	3.74	3.42	3.59	3.55	3.81	3.83	3.63	3.97

Table 4-6: Wire pull and die shear for 150 C experiments and control devices. Die shear is in kilograms force, wire pull is in grams force.

Test Condition	**150 C 100 hr**		**150 C 500 hr**		**Controls**		
Package ID	**1232**	**1236**	**1222**	**1242**	**5040**	**1215**	**1245**
Die Shear	21.4	18.2	22.6	26.5	23.5	29.9	20.7
Min wire pull	2.71	2.85	2.47	2.42	2.98	2.59	2.30
Max wire pull	4.04	4.48	3.92	4.02	5.00	4.07	4.39
Average pull	3.23	3.58	3.03	3.22	3.96	3.33	3.17

All of the wire pull and die shear tests passed the MIL-STD-883 minimum requirements, and there were no observable trends based on time or temperature.

The packages were also shear tested on the printed circuit board to determine if they were properly adhered. In all cases, the maximum load of 100 kilograms was applied without shearing the package off the board.

5. Conclusions

All of the aged shock sensor devices passed functionality testing, and all sampled parts passed die shear and wire bond pull test requirements. There were two packages that showed anomalous measurements in the residual gas analysis, with high levels of water, oxygen, and argon present. The reason for this difference is currently unknown, but it did not affect any other performance metrics. Assuming an apparent activation energy of 0.7 eV, this experiment has exposed the shock sensor device to an accelerated aging condition of 20 years without failure.

6. References

[1] Mitchell, J.A., Alvares, M., Baker, M.S., Spletzer, M.A. and Tanner, D.M., "The Sandia MEMS Passive Shock Sensor: FY09 Maturation Activities Reaching TRL 5+," Sandia Report SAND2009-7652, printed November 2009.

[2] JEDEC Publication, “Failure Mechanisms and Models for Semiconductor Devices,” JEP122E, *JEDEC Solid State Technology Association*, March 2009.

Distribution List

All Distribution will be by electronic copy only

Copies	Mail Stop	Recipient	Organization
1	1310	Michael Baker	1749-1
1	1322	John A. Mitchell	1435
1	0525	Danelle Tanner	1732
1	1080	Keith Ortiz	1749
1	1064	Joel Wirth	2614
1	0899	Technical Library	9536 (electronic copy)